

## ScGaN alloy growth by molecular beam epitaxy: Evidence for a metastable layered hexagonal phase

Costel Constantin, Hamad Al-Britthen, Muhammad B. Haider, David Ingram, and Arthur R. Smith\*

Condensed Matter and Surface Science Program, Department of Physics and Astronomy, Ohio University, Athens, Ohio 45701, USA

(Received 5 October 2003; published 23 November 2004; publisher error corrected 8 December 2004)

Alloy formation in ScGaN is explored using rf molecular beam epitaxy over the Sc fraction range  $x=0-100\%$ . Optical and structural analysis show separate regimes of growth, namely (I) wurtzitelike but having local lattice distortions in the vicinity of the  $\text{Sc}_{\text{Ga}}$  substitutions for small  $x$  ( $x \leq 0.17$ ), (II) a transitional regime for intermediate  $x$ , and (III) cubic, rocksaltlike for large  $x$  ( $x \geq 0.54$ ). In regimes I and III, the direct optical transition decreases approximately linearly with increasing  $x$  but with an offset over region II. Importantly, it is found that for regime I, an anisotropic lattice expansion occurs with increasing  $x$  in which  $a$  increases much more than  $c$ . These observations support the prediction of Farrer and Bellaiche [Phys. Rev. B **66**, 201203-1 (2002)] of a metastable layered hexagonal phase of ScN, denoted  $h$ -ScN.

DOI: 10.1103/PhysRevB.70.193309

PACS number(s): 78.66.Fd, 61.14.Hg, 61.66.Dk, 68.55.Nq

ScN is a rocksalt (cubic) semiconductor with an indirect band gap from  $\Gamma \rightarrow X$  of  $\sim 1$  eV and a direct transition  $E_i$  at the X point of 2.1–2.4 eV.<sup>1–6</sup> It is interesting to investigate the possibility of nitride band gap engineering by putting Sc into GaN.<sup>7</sup> Takeuchi predicted a metastable wurtzite phase ( $w$ -ScN) for ScN.<sup>8</sup> However, recently Farrer and Bellaiche have found that  $w$ -ScN should be unstable and that instead a layered hexagonal phase having nearly fivefold coordination, denoted  $h$ -ScN, which can be arrived at by flattening the bilayer of the wurtzite structure, should be metastable.<sup>9,10</sup> In fact, such a structure has also been predicted to exist for MgO ( $h$ -MgO).<sup>11</sup> Yet, aside from the report of Little and Kordesch, who grew ScGaN by sputtering and reported amorphous or microcrystalline films and a linearly decreasing optical band gap (from 3.5 down to 2.0 eV) with increasing Sc concentration,<sup>12</sup> little is known experimentally regarding the actual crystal structures of ScGaN alloys. For example, one might expect more than one growth regime for crystalline films. If so, then novel transitional properties, as suggested by Farrer and Bellaiche, might be observed at the boundary between the two different regimes.<sup>9</sup>

In this Brief Report, we present results for ScGaN film growth using a custom molecular beam epitaxy (MBE) system that employs Ga and Sc effusion cells and a rf plasma N source. The sapphire (0001) substrates are first nitrated at 650 °C for 15 min with N plasma source operating at 500 W with a  $\text{N}_2$  flow rate of 1.1 sccm ( $P_{\text{chamber}}=9 \times 10^{-6}$  Torr). The ScGaN is then grown at specific flux ratio  $r=J_{\text{Sc}}/(J_{\text{Sc}}+J_{\text{Ga}})$  at 650 °C to a thickness of 250–340 nm. The N flux is held constant with growth under N-rich conditions ( $J_{\text{Sc}}+J_{\text{Ga}} < J_{\text{N}}$ ). The growth is monitored *in situ* by reflection high energy electron diffraction (RHEED) using a 20 KeV  $e^-$ -beam, and the films are studied *ex situ* by x-ray diffraction (XRD) with Cu  $K\alpha$  x rays, optical absorption (OA), and Rutherford backscattering (RBS).

A series of ScGaN films on sapphire (0001) with  $r$  in the range between 0 and 1 have been grown and analyzed. Presented in Fig. 1 are the RHEED patterns of 8 such ScGaN films, including the two endpoints at  $r=0$  [GaN(000 $\bar{1}$ )] and

$r=1$  [ScN(111)]. The direction of the RHEED beam is along  $[11\bar{2}0]$  for GaN and correspondingly  $[1\bar{1}0]$  for ScN.

Calculation of the RHEED patterns is accomplished by considering the structural models. Figure 2(a) shows a side-view model of the  $[000\bar{1}]$ -oriented wurtzite GaN bi-layers as viewed along  $[11\bar{2}0]$ , and Fig. 2(b) shows the associated reciprocal space map with spot indices  $\nu_1 \nu_2 \nu_3$ . The intensity of the diffraction spots with  $\nu_1$  odd, calculated from the structure factor for wurtzite, alternates along the  $k_z$  direction, and the spots with  $\nu_1=0$  and  $\nu_3$  odd have zero intensity. Clearly the RHEED pattern of GaN(000 $\bar{1}$ ) shown in Fig. 1(a) is in good agreement with the calculated reciprocal space map, and the measured ratio of  $S_{\text{in,GaN}}$  to  $S_{\text{out,GaN}}$  for GaN is 1.92, which agrees well with the expected value  $c/(\sqrt{3}a/2) = 5.185 \text{ \AA}/2.762 \text{ \AA} = 1.877$ .

Figure 2(c) shows the side-view model of ScN(111) as viewed along  $[1\bar{1}0]$  together with the corresponding reciprocal space map shown in Fig. 2(d). The spot intensities are calculated from a superposition of the structure factors of two inequivalent 111-oriented fcc grains (note that fcc is not two-fold symmetric about 111, and for a single grain the diffraction pattern is asymmetrical about the 00 rod). Clearly the RHEED pattern of ScN(111) shown in Fig. 1(e) is in excellent agreement with the calculated reciprocal space map in Fig. 2(d), and the ratio of the lateral spot spacing  $S_{\text{in,ScN}}$  to  $S_{\text{out,ScN}}$  is measured to be 2.86, in good agreement with the expected value of  $2\sqrt{2} \approx 2.83$ .

Comparing the rocksalt and wurtzite patterns, we note that the measured spacing  $S_{\text{out,ScN}}$  [see Fig. 1(e)] is very close to  $2\times$  the measured spacing  $S_{\text{out,GaN}}$  [see Fig. 1(a)], due to the fact that the Sc layer spacing  $a/\sqrt{3}=2.599 \text{ \AA}$  in ScN is very close to the Ga layer spacing  $c/2=2.592 \text{ \AA}$  in GaN. Yet clearly the RHEED patterns of wurtzite and rocksalt are easily distinguishable.

Shown in Figs. 1(b)–1(d) are the RHEED patterns for ScGaN alloy films having  $r$  in the range  $0 < r \leq 0.29$ . These RHEED patterns are in good agreement with the wurtzite reciprocal space map. However, we note that the structure

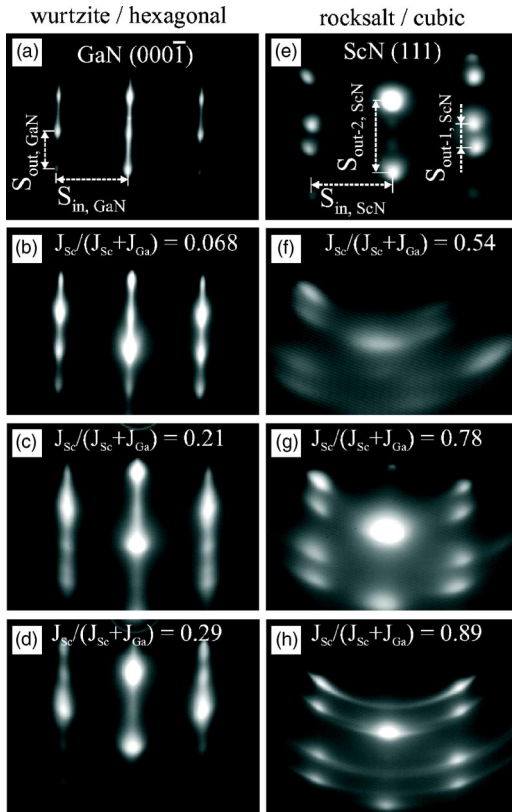


FIG. 1. (a) RHEED pattern of wurtzite GaN(000 $\bar{1}$ ) along  $[11\bar{2}0]$ ; (b)–(d) RHEED patterns of  $\text{Sc}_x\text{Ga}_{1-x}\text{N}$  for low Sc concentration along same azimuth as (a); (e) RHEED pattern of rocksalt ScN(111) along  $[1\bar{1}0]$ ; (f)–(h) RHEED pattern of  $\text{Sc}_x\text{Ga}_{1-x}\text{N}$  for high Sc concentration along the same azimuth as (e).

factor for the layered hexagonal phase is identical to that of wurtzite. To determine if these ScGaN samples are consistent with wurtzite or not, it is necessary to consider the measured lattice constants  $a$  and  $c$  (discussed below).

Shown in Figs. 1(f)–1(h) are the RHEED patterns for ScGaN films having  $r$  in the range  $0.54 \leq r < 1$ . Although each pattern shows a degree of polycrystallinity (based on the ringlike RHEED pattern), each pattern is in good agreement with the rocksalt-type pattern shown in Figs. 1(e) and 2(d). The results suggest that each monocrystal has rocksalt structure for growth at large Sc composition, consistent with predictions.<sup>9,13</sup>

Incorporation  $x \equiv N_{\text{Sc}}/(N_{\text{Sc}} + N_{\text{Ga}})$ , where  $N_{\text{Sc}}$  and  $N_{\text{Ga}}$  are the number of Sc and Ga atoms within a given volume, respectively, was obtained using RBS; the results are given in Table I. Whereas  $r$  and  $x$  are about the same for the cubic regime ( $r \geq 0.54$ ), for the hexagonal regime ( $r \geq 0.29$ ),  $x$  is consistently smaller than  $r$ , suggesting that the sticking coefficients  $S_{\text{Ga}}$  and  $S_{\text{Sc}}$  are different at low  $r$  values but similar at high  $r$  values. This behavior is reasonable given that the N-polar (and N-terminated) wurtzite like surface would have a single dangling bond per N atom (film polarity is determined in a later experiment by the RHEED pattern after subsequent growth of a GaN layer under Ga-rich conditions).<sup>14,15</sup> In comparison, from the model of Fig. 2(c), the (111)-oriented, N-terminated rocksalt surface would have

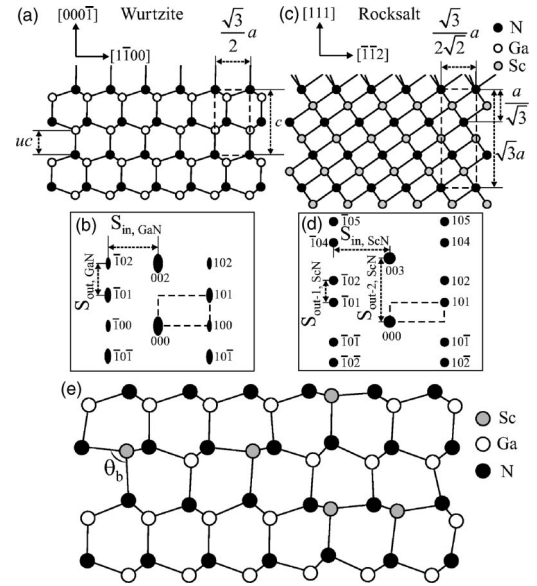


FIG. 2. (a) Side-view diagram of GaN[000 $\bar{1}$ ] along  $[11\bar{2}0]$ ; (b) reciprocal space map corresponding to (a), 3-index notation corresponds to  $\nu_1 \nu_2 \nu_3$  which label the reciprocal-lattice points; (c) side-view diagram of ScN[111] along  $[1\bar{1}0]$ ; (d) reciprocal space map corresponding to (c) using similar 3-index notation. Size of dots is proportional to their intensity; (e) schematic model of ScGaN for low  $x$  regime showing local distortions of the bond angle  $\theta_b$ .

3 dangling bonds per N atom, resulting in larger surface diffusion barrier of both Sc and Ga atoms, rougher growth mode, and larger sticking coefficients for both Sc and Ga. This agrees with the RHEED patterns which are more spotty for the cubic regime compared to the hexagonal regime.

The lattice constant  $a$  is directly obtained from the RHEED pattern using a peak fitting program. The RHEED calibration is performed using a GaN substrate grown by metal-organic chemical vapor deposition. The resulting  $a$  values are plotted vs  $x$  in Fig. 4 for the small  $x$  values, where it is seen that  $a$  increases with  $x$ .

Crystallinity and *out-of-plane* lattice constant information was determined using XRD, and shown in Fig. 3 are results for ScGaN layers with low  $x$ . Figure 3(a) shows the entire XRD spectrum ( $20^\circ - 140^\circ$ ) for the film with  $x=0.05$  where 5 peaks are seen—2 sapphire peaks (0006 and 00012) and 3 ScGaN peaks (0002, 0004, and 0006). The spectra are corrected so that both sapphire peaks give the same lattice constant ( $c=12.98 \text{ \AA}$ ); the alignment of the sapphire 0006 peaks for films with  $x=0.05$ , 0.14, and 0.17 is presented in Fig. 3(b). The observed ScGaN peak shift for the same 3 samples is shown in Fig. 3(c); compared to  $x=0$ , the 0002 peak shifts to the left for  $x=0.05$  and 0.14 but interestingly shifts slightly back to the right for  $x=0.17$ , from which the  $c$ -spacings are calculated using Gaussian peak fitting and Bragg's law to be 5.190  $\text{\AA}$ , 5.195  $\text{\AA}$ , and 5.194  $\text{\AA}$ , respectively, compared to 5.188  $\text{\AA}$  for  $x=0$ . The  $c$  values are also plotted in Fig. 4 vs  $x$ .

Over the range  $0 < x < 0.17$ ,  $a$  increases by a net 0.08  $\text{\AA}$  while  $c$  increases by only a net 0.006  $\text{\AA}$ . Thus for the small  $x$  range, the  $\text{Sc}_x\text{Ga}_{1-x}\text{N}$  lattice expands predominantly within

TABLE I. Flux ratio  $r=J_{\text{Sc}}/(J_{\text{Ga}}+J_{\text{Sc}})$ , Sc composition  $x=N_{\text{Sc}}/(N_{\text{Sc}}+N_{\text{Ga}})$ , XRD 0002 peak amplitude, XRD 0002 FWHM, RHEED FWHM, measured  $c/a$  ratio, expected  $c/a$  ratio (based on Ref. 17), and  $c/a$  ratio for ideal wurtzite structure (based on Ref. 13 for different  $\text{Sc}_x\text{Ga}_{1-x}\text{N}$  samples). Samples 1–4 correspond to regime I, samples 5–7 to regime III.

ScGaN sample	1	2	3	4	5	6	7
Flux ratio $r$	0	0.068	0.21	0.29	0.54	0.78	0.89
Composition $x$	0	0.05	0.14	0.17	0.54	0.74	0.89
0002 XRD peak ampl.	82182	51443	13086	5438			
0002 XRD FWHM	0.149°	0.181°	0.277°	0.349°			
RHEED FWHM	8.1	9.7	19.4	22.6			
Measured $c/a$	1.635	1.621	1.612	1.595			
$c/a$ expected based on Ref. 17	1.626	1.62	1.60	1.60			
Ideal wurtzite $c/a$ based on Ref. 13	1.62	1.62	1.61	1.61			

the  $c$ -plane. Such anisotropic expansion as well as the decrease of  $c$  between  $x=0.14$  and  $0.17$  would not be expected in the case of alloying of isocrystalline binary compounds. The anisotropic expansion suggests the following picture, as illustrated by the schematic model shown in Fig. 2(e): at the location where a Sc atom substitutes for a Ga atom, a local lattice distortion occurs in which the N-Sc-N bond angle  $\theta_b$  (having one leg in the  $c$ -direction) reduces compared to the  $\sim 109^\circ$  for a wurtzite bond (in ideal  $h$ -ScN,  $\theta_b=90^\circ$ ). In other words, the internal parameter  $u$  [see Fig. 2(a)] varies within the alloy away from the  $w$ -GaN value  $0.376$ .<sup>9</sup> For  $h$ -ScN ( $x=1$ ), Farrer *et al.* have predicted  $a=3.66$  Å,  $c=4.42$  Å, and  $c/a=1.207$ .<sup>9</sup> Thus  $a$  can potentially locally increase by up to 14.77% of  $a_{\text{GaN}}=3.189$  Å, depending on  $x$ ; at the same time,  $c$  would locally decrease.<sup>16</sup>

Further experimental evidence for the low  $x$  regime points to the same model. First, we note substantial broadening of the RHEED diffraction lines with increasing  $x$  (see FWHM

values vs  $x$  in Table I). Second, we note the substantial intensity decrease and broadening of the 0002 ScGaN XRD peak with increasing  $x$  [see Fig. 3(c) and also Table I]. Such behavior is indicative of an increased spread of lattice constants with increasing  $x$ , resulting in reduction of the long range order or of the maximum correlation length of the crystal.

Very recently, Ranjan and Bellaiche have calculated the  $c/a$  ratio for an ideally ordered  $\text{Sc}_x\text{Ga}_{1-x}\text{N}$  having  $x=0.5$  to be 1.55.<sup>17</sup> Considering the  $c/a$  ratio for GaN ( $x=0$ ) to be  $1.626=5.185$  Å/ $3.189$  Å, linear interpolation gives decreasing values of  $c/a$  for increasing  $x$ . These data are presented in Table I which also shows values for the ideal wurtzite  $c/a$  ratios vs  $x$  (based on Ref. 13). The data show that the change in  $c/a$  over the range  $x=0$  to  $0.17$  is  $-0.01$  for the wurtzite case versus  $-0.03$  for the model of Ranjan and Bellaiche. The experiment, which finds a change in  $c/a$  over this range to be  $-0.040$ , is thus in better agreement with the latter.

Extrapolating straight line fits of the measured  $a$  and  $c$  vs  $x$  data to  $x=1$  results in  $a(x=1)=3.60$  Å  $c/a=1.45$  for a hypothetical ScN in hexagonal phase. Thus the extrapolated  $c/a$  ratio is significantly smaller than that predicted for  $w$ -ScN (1.6); and, the extrapolated  $a$  is significantly larger than that predicted for  $w$ -ScN (3.49 Å),<sup>8</sup> closer in fact to the value predicted for  $h$ -ScN (3.66 Å).<sup>9</sup> In fact, we note that  $a$  increases faster, and that  $c$  decreases, with  $x$  between 0.14 and 0.17.

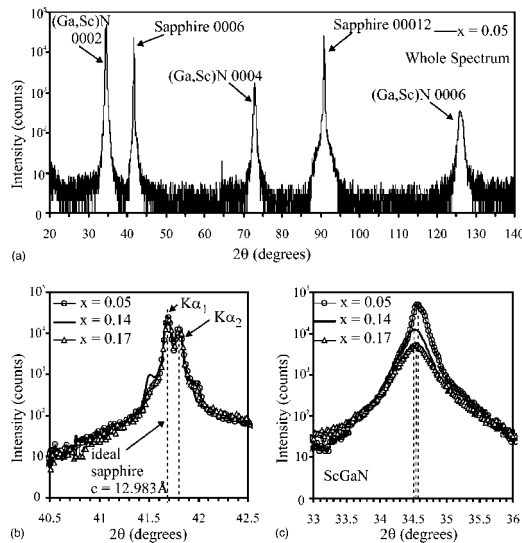


FIG. 3. (a) XRD of a representative spectrum with  $x=0.05$  showing the two sapphire peaks [0006 and 00012] and three ScGaN peaks [0002, 0004, and 0006]; (b) sapphire 0006 peaks for the films with  $x=0.05, 0.14, 0.17$ ; (c) ScGaN 0002 peaks at  $2\theta\sim 34.5^\circ$  for the films with  $x=0.05, 0.14, 0.17$ .

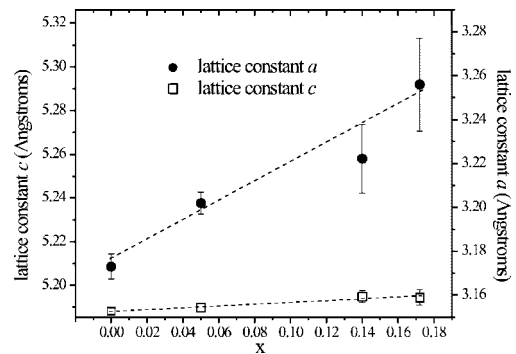


FIG. 4. The lattice spacings  $a$  and  $c$  vs  $x$  for low Sc concentration.

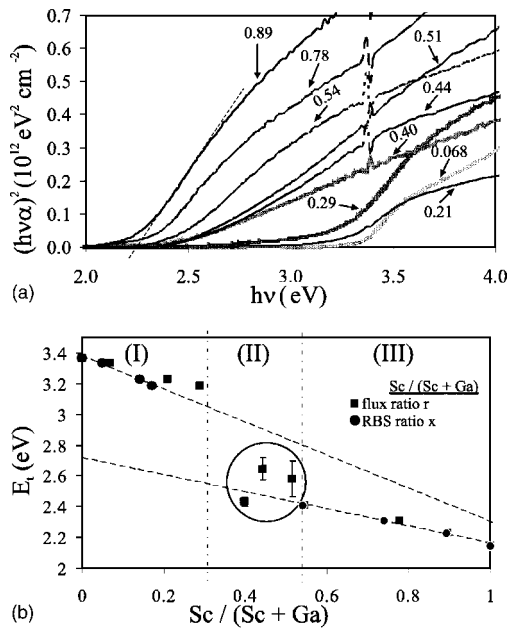


FIG. 5. (a) Optical absorption measurements of all the films; numbers are the  $\text{Sc}/(\text{Sc} + \text{Ga})$  flux ratios  $r$ , and tangent line for  $r = 0.89$  exemplifies method of obtaining  $E_t$ . Small peaks at  $\sim 3.4$  eV for large  $x$  are instrumental in origin and of no importance here. (b) Deduced  $E_t$  values vs  $r$  and  $x$  for all the films showing the 3 different regions. Most error bars are too small to be seen.

Optical absorption measurements have been obtained for all the films. Shown in Fig. 5(a) is plotted the quantity  $(h\nu\alpha)^2$  vs  $h\nu$  for each film. The  $E_t$  is estimated from the energy intercept of a straight line tangent to the curve near its inflection point. The resulting  $E_t$  values are plotted vs  $r$  and  $x$  in Fig. 5(b). The  $E_t = 3.37$  eV of wurtzite GaN is obtained at  $x = 0$ . The  $E_t = 2.15$  eV is obtained at  $r = 1$  for ScN grown on MgO(001).<sup>5</sup> As can be seen, three different regions, consis-

tent with the RHEED results, can be distinguished: (I) low Sc fraction ( $0 < r < 0.30$ ); (II) intermediate Sc fraction—transitional regime ( $0.30 < r < 0.54$ ); and (III) high Sc fraction ( $0.54 < r < 1$ ). In both regions I and III,  $E_t$  decreases monotonically with increasing  $x$ .

For region I, extrapolating a straight line fit of the  $E_t$  values to  $x = 1$  (pure ScN) obtains an  $E_t = 2.3$  eV—significantly smaller than the value of  $\sim 3.0$  eV predicted for the  $E_t$  of  $w$ -ScN.<sup>8</sup> The extrapolation from low  $x$  however is probably not a good estimate of the  $E_t$  of  $h$ -ScN since layered hexagonal is not iso crystalline with the low  $x$  regime (wurtzite with local N-Sc-N bond distortions).

As RHEED indicates, rocksalt structure is observed for larger  $x$  (region III), and within region III,  $E_t$  decreases linearly towards the rocksalt value of 2.15 eV at  $x = 1$ . Using a straight line fit to the  $E_t$  values of region III and extrapolating to  $x = 0$  yields an  $E_t = 2.72$  eV for a hypothetical GaN in rocksalt structure. Finally, the  $E_t$  values in region II (encircled points) with  $r$  in the range 0.30–0.51 show comparatively large variations, which are consistent with the expected instability of the crystal structure near the transition between the stable hexagonal and cubic regimes.

To summarize, we have shown that the disparate ground state crystal structures of ScN and GaN lead to two distinct regimes of structural and optical properties. For both low  $x$  and high  $x$ , alloy-type behavior is observed. For  $x \geq 0.54$ , rocksalt structure is found, in agreement with predictions.<sup>9,13</sup> For small  $x$  up to 0.17, an anisotropic expansion of the ScGaN lattice is observed which is interpreted in terms of local lattice distortions of the wurtzite structure in the vicinity of  $\text{Sc}_{\text{Ga}}$  substitutional sites in which there is a decrease of the N-Sc-N bond angle. This tendency toward flattening of the wurtzite bilayer is consistent with a predicted  $h$ -ScN phase.<sup>9</sup>

This work was supported by the National Science Foundation under Grant No. 9983816.

\*Author to whom correspondence should be addressed. Electronic address: smitha2@ohio.edu

<sup>1</sup>P. Dismukes *et al.*, J. Cryst. Growth **13/14**, 365 (1972).

<sup>2</sup>D. Gall *et al.*, J. Vac. Sci. Technol. A **16**, 2411 (1998).

<sup>3</sup>D. Gall *et al.*, J. Appl. Phys. **84**, 6034 (1998).

<sup>4</sup>T. D. Moustakas *et al.*, Proc.-Electrochem. Soc. **96-11**, 197 (1996).

<sup>5</sup>A. R. Smith *et al.*, J. Appl. Phys. **90**(4), 1809 (2001).

<sup>6</sup>H. A. AL-Brithen *et al.*, Phys. Rev. B **70**, 045303 (2004).

<sup>7</sup>J. P. Dismukes and T. D. Moustakas, Proc.-Electrochem. Soc. **96-11**, 110 (1996).

<sup>8</sup>N. Takeuchi, Phys. Rev. B **65**, 045204 (2002).

<sup>9</sup>N. Farrer and L. Bellaiche, Phys. Rev. B **66**, 201203 (2002).

<sup>10</sup>V. Ranjan *et al.*, Phys. Rev. Lett. **90**, 257602 (2003).

<sup>11</sup>S. Limpijumong and W. R. L. Lambrecht, Phys. Rev. B **63**, 104103 (2001).

<sup>12</sup>M. E. Little and M. E. Kordesch, Appl. Phys. Lett. **78**, 2891 (2001).

<sup>13</sup>M. G. Moreno-Armenta *et al.*, Phys. Status Solidi B **238**, 127 (2003).

<sup>14</sup>A. R. Smith *et al.*, Appl. Phys. Lett. **72**, 2114 (1998).

<sup>15</sup>A. R. Smith *et al.*, Phys. Rev. Lett. **79**, 3934 (1997).

<sup>16</sup>Tosja Zywiwicz *et al.*, Appl. Phys. Lett. **73**, 487 (1998).

<sup>17</sup>V. Ranjan and L. Bellaiche (unpublished).